Nanocatalysts from Ionic Liquid Precursors for the Direct Conversion of CO_2 to Hydrocarbons

Callum Jeffrey[1], Peter Nockemann[1], Nancy Artioli[1*]
[1] *School of Chemistry and Chemical Engineering, Queen's University Belfast, Belfast, UK*

**corresponding author:n.artioli@qub.ac.uk*

Introduction

The direct conversion of carbon dioxide (CO_2) into lower olefins (C_2-C_4) is a highly desirable process as a sustainable production route. Lower olefins, i.e., ethylene, propylene and butenes (C_2-C_4), are key building blocks in the current chemical industry. The reaction proceeds *via* two main consecutive reactions: Reverse Water Gas Shift (RWGS) to produce CO followed by the further conversion of CO to hydrocarbons *via* the Fischer−Tropsch reaction[2]. This process is achieved by a multifunctional iron-based catalyst supported on zeolites providing three types of active sites (Fe_3O_4, Fe_5C_2 and acid sites), which cooperatively catalyse a tandem reaction[1].

To date, attempts at synthesising a suitable catalyst for the direct hydrogenation reaction follow a conventional precipitation procedure, whereby Iron Oxide Nanoparticles (*IONs*) are produced and then embedded within a zeolite structure by granule mixing. This method provides no control over the size and shape of the IONs formed; a characteristic of imperative importance due to its significant effect on the hydrocarbon product distribution obtained. In our novel approach, ionic liquids are utilised for the synthesis of the *IONs* resulting in better control over size and morphology of the nanostructured material, and as a consequence, better conversion and selectivity towards the olefins.

Materials and Methods

Na–Fe_3O_4 nanocatalysts obtained by a one-pot synthesis method employing a precipitation method involving a mixture of iron (II) and iron (III) chloride hydrate, deionised water and HCl to result in a clear solution. Subsequently, NaOH has been added as a precipitating agent, which resulted in the formation of a black precipitate, which consisted of magnetite, Fe_3O_4. The compound was then characterised using IR, PXRD (see Fig. 1), SEM / EDX and TPR (Fig. 2). Depending on the amount of washing water, the catalyst contained varying amounts of residual sodium content of up to $7{\cdot}10^{-2}$ %.

The ionic liquid-assisted synthesis involved heating the reaction medium consisting of the ionic liquid 1-butyl-3-methyl imidazolium bistriflimide, [C_4mim][Tf_2N], oleic acid and iron pentacarbonyl under reflux. The precursor iron pentacarbonyl decomposed in a controlled manner by heating the sample up; CO is produced and the iron reacts with residual H_2O in the ionic liquid mixture to result in Fe_3O_4. Following decomposition, the produced magnetite nanoparticles are separated from the reaction medium through application of a neodymium magnet. The Na–Fe_3O_4/Zeolite catalyst was typically prepared by granule mixing Na–Fe_3O_4 catalysts prepared with the methods above with zeolites (HZSM(SiO_2/Al_2O_3 = 80 and 300) in a ball mill at a mass ratio of the two components of 1:1.

CO_2 hydrogenation reactions were performed at 320 °C, 3 MPa H /CO 3,3 in a stainless steel fixed-bed reactor with an inner diameter of 15 mm. Typically,1 g of composite catalyst (20–40 meshes) with Na–Fe_3O_4/Zeolite ¼ 1/1 (mass ratio) was used. Prior to reaction, the catalyst was in-situ reduced at 350 °C for 8 h in a pure H_2 flow at atmospheric pressure.

All of the products from the reactor were introduced in a gaseous state and analysed with a online gas chromatograph (GC).

Results and Discussion

The ionic-liquid assisted synthesis of a nanocrystalline magnetite precursor showed that ionic liquids provide a controlled precipitation method thanks to their dual functionality as solvent and templating agent. This level of control over the morphology of the produced IONs allows for the selectivity of the hydrocarbon distribution to be directly tailored to light olefin production. Characterization of the prepared catalysts by PXRD (Figure 1) shows phase purity for the magnetite obtained from the conventional precipitation method, and shows no alteration after granulation with the zeolite, showing the presence of high purity in Fe_3O_4, small particle size and good dispersion with the zeolite component. The compounds obtained by the ionic liquid methods result in much broader XRD patters, pointing at less crystallinity and smaller particle size. This has also been confirmed by SEM and TEM. Hydrogen temperature-programmed reduction (H_2-TPR) was used to determine the interaction between Fe species and the support. As shown in Figure 2 for the HZSM 80, all the catalysts present two peaks with increasing reduction temperature, which are assigned to the conversions Fe_3O_4—FeO and FeO—Fe, respectively. It is observed that Fe_3O_4/HZSM80 start to be reduced at lower temperature compared to the catalyst with low (l) and high (H) Na content. This indicates the interaction between iron oxides and the support is weaker if Na is completely removed .

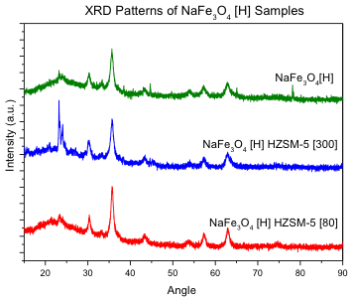

Figure 1. XRD patterns of Na–Fe_3O_4 sample with high Na content (H) and Na–Fe_3O_4 mixed with HZSM with SiO_2/Al_2O_3 = 80 and 300.

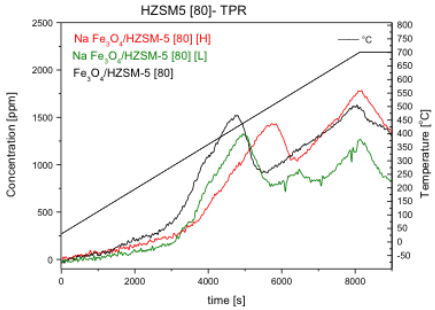

Figure 2. TPR profile of 4000 ppm H_2 in Ar from r.t. to700ºC, 5ºC/min

Significance

We report here on a novel methodology for the controlled synthesis of a Na–Fe3O4/HZSM-5 multifunctional catalyst for the direct hydrogenation of CO_2 to gasoline. The catalytic testing under industrially relevant conditions resulted in improved selectivity to C5–C11 as well as low CH_4 and CO selectivity. Furthermore, the product composition can be tuned by the choice of zeolite type, and by the choice of ionic liquid in the synthetic method. This study provides a new pathway for the synthesis of nanocatalysts for the production of liquid fuels by utilising CO_2 and H_2, which may in the future lead to alternative approaches to overcome issues with the intermittency of storing and/or utilising energy from renewable sources (photovoltaics, wind energy).

References

[1]Y. Yuan, S. Huang, H. Wang, Y. Wang, J. Wang, J. Lv, Z. Li, and X. Ma, ChemCatChem 2017, 9, 3144 – 3152

[2] J. Wei, Q. Ge, R. Yao, Z. Wen, C. Fang, L. Guo, H. Xu, J. Sun, Nat Comm, DOI: 10.1038/ncomms15174

UKCC 2019

List of Orals 2019

#	Title	Authors
PI01	Design and implementation of *de novo* biosynthetic cascades	Sabine Flitsch
PI02	Process intensification through structuring catalyst and reactor - Highly active Fischer-Tropsch synthesis catalysts by MOF mediated synthesis	Freek Kapteijn, Xiaohui Sun, Tim Wezendonk, David Vervloet, Bart Kaskes, Ruud van Ommen and Jorge Gascon
PI03	Design of stable Ni/ZrO2 catalysts for methane dry reforming	Andreas Jentys, M. Steib, Y. Lou, Y. Liu, J. A. Lercher
PI04	Computer-aded Design of Sulfide Nano-catalysts for Sustainable Energy Applications	Nora H. de Leeuw
K01	Can Base Metals Replace PGMs in Catalysts for Three-way Gasoline Emissions Control? Kinetic, Reaction Mechanism and Catalyst Sizing	Andrew York, Crispin Cooper, Kerry Simmance and Sam Wilkinson
	Biocatalyst – artificial metalloenzyme cascade based on alcohol dehydrogenase	Simone Morra and Anca Pordea
K02	A chemo-enzymatic oxidation cascade to activate C–H bonds with in situ generated H2O2	Simon Freakley
K03	Developing “Strong and Stable” Palladium Catalysts for Wacker-Type Oxidation Reactions	Mark Muldoon and Matthew Blair
K04	Molecular insights into the enzymatic oxidation of polysaccharides by lytic polysaccharide monooxygenases	Paul Walton and Gideon Davies
K05	From Lignin to Chemicals: Hydrogenation of Lignin Models and Mechanistic Insights into Hydrodeoxygenation via Low Temperature C–O Bond Cleavage	George Britovsek
K06	Direct Correlation between Adsorption Energetics and Nuclear Spin Relaxation in a Liquid-saturated Catalyst Material	Carmine D'Agostino, Neil Robinson, Christopher Robertson, Lynn Gladden and Stephen Jenkins
K07	Fischer-Tropsch – An Old Technology with New Opportunities	James Paterson

K08	Structure Selectivity of Supported Pd nanoparticles for Catalytic NH3 Oxidation resolved using combined Operando Spectroscopy	Ellie K. Dann, Emma K. Gibson, Rachel H. Blackmore, C. Richard A. Catlow, Paul Collier, Arunabhiram Chutia, Tugce Eralp Erden, Christopher Hardacre, Anna Kroner, Maarten Nachtegaal, Agnes Raj, Scott M. Rogers, S. F. Rebecca Taylor, Paul Thompson, George F. Tierney, Constantinos D. Zeinalipour Yazdi, Alexandre Goguet and Peter P Wells
K09	Spatially orthogonal chemical functionalization of a hierarchical pore network for catalytic cascade reactions	Christopher Parlett, Mark Isaacs, Simon Beaumont, Karen Wilson and Adam Lee
K10	Biocatalyst – artificial metalloenzyme cascade based on alcohol dehydrogenase	Simone Morra and Anca Pordea
K11	Magnetocatalysis for selectivity manipulation	Pip Hellier, Michael Bowker, Adli Peck and Michael Claeys
K12	Mechanistic Insights into the Liquid Phase Hydrogenation/Deuteration of Mandelonitrile	Mairi McAllister, Cédric Boulho, Colin Brennan and David Lennon
K13	Cross-checking typical Langmuir-Hinshelwood model assumptions with direct liquid-phase adsorption studies	Nikolay Cherkasov, Alexander Kunitsa, David Jackson and Evgeny Rebrov
O01	Low Temperature NOx Storage on Pd zeolites for low temperature cold start emissions	Maria Pia Ruggeri, Loredana Mantarosie and Husn Islam
O02	Selective Catalytic Reduction of NO with NH3 over Cu, Fe-Zeotype Catalysts: Operando Synchrotron IR Microspectroscopic Study	Ivalina Minova, Paul Wright, Alex Greenaway, Andrew Beale, Russell Howe, Santhosh Matam, Mark Frogley and Gianfelice Cinque
O03	OMS-2 molecular sieves doped with ceria for the development of new emission control catalysts	Kathryn Rogers, Ruairi O'Donnell, Maxime Grolleau, John Duffin, Haresh Manyar, Nancy Artioli
O04	Towards Application of Prenylated Flavin-dependent Decarboxylase	Godwin Aleku and David Leys
O05	Simulation as an Aid for Biocatalyst Engineering: Insights, Tools and In Silico Assays	Marc van der Kamp, Sam Johns and Stefano Serapian
O06	Electro-catalytic reduction of CO2 to acetic acid on greigite Fe3S4	David Santos-Carballal, Alberto Roldan Martinez and Nora H. de Leeuw

O07	Effect of NOx on the Capture and Utilisation of CO2 in Superbase Ionic Liquids	Adam Greer, Rebecca Taylor, Helen Daly, Christopher Hardacre, Johan Jacquemin, Matthew Quesne and Richard Catlow
O08	Selectivity of CO2 photoelectrochemical reduction on Ag, Bi tungstates	Miguel Galante, Mohammad Hossain, Paola Munoz, Luis Duarte, Rebecca Taylor, Christopher Hardacre, Robin Macaluso, Krishnan Rajeshwar and Claudia Longo
O09	Is there an Alternative to the Haber-Bosch process? An ab-initio Analysis of the Catalytic Oxidation of Nitrogen	Ulrich Hintermair, Vera Krewald and Jack Glancy
O10	Au-Pd alloy catalysts for the oxidation of organic compounds	Ali Nasrallah, David Willock and Richard Catlow
O11	Total Neutron Scattering integrated with NMR to Study Heterogeneous Catalysis	Markus Leutzsch, Marta Falkowska, Terri-Louise Hughes, Andrew J. Sederman, Lynn F. Gladden, Michael D. Mantle, Tristan G. A. Youngs, Daniel T. Bowron, Haresh Manyar and Chris Hardacre
O12	Recent Developmetns in Asymmetric Reduction using Ruthenium Catalysts	Martin Wills
O13	Towards a Mechanistic Understanding of Antimicrobial Resistance to Colistin	Reynier Suardiaz, Emily Lythell, Philip Hinchliffe, Natalie Fey, James Spencer and Adrian Mulholland
O14	Constrained geometry complexes for ethylene polymerisation catalysis	Thomas Williams, Jean-Charles Buffet, Alexander Smith, Zoë Turner and Dermot O'Hare
O15	Influence of catalyst aging on the low-temperature interactions of 1-octene with ZSM-5 cracking catalyst: a neutron spectroscopic study.	Alexander Hawkins, Alexander O'Malley, Andrea Zachariou, Paul Collier, Russell Ewings, Ian Silverwood, Russell Howe, Stewart Parker and David Lennon
O16	ULTRA laser facility: what we can offer to the catalysis community	Igor Sazanovich, Gregory Greetham, Ian Clark, Paul Donaldson and Michael Towrie
O17	Using Inelastic Neutron Scattering to Study the Changing Nature of the ZSM-5 Catalyst during the Methanol-to-Hydrocarbons Reaction	Andrea Zachariou, Alexander Hawkins, Suwardiyanto, Russell Howe, Paul Collier, Stewart F. Parker and David Lennon
O18	Molecularly Imprinted Polymers for the Recovery and Recycling of Thio(urea) organocatalysts	Federica Pessagno, Matthew Blair, Mark Muldoon and Panagiotis Manesiotis
O19	Killing Two Birds with One Stone: Organocatalytic Membrane Reactor for Integrated Synthesis and Separation	Levente Cseri, Jozsef Kupai and Gyorgy Szekely

UKCC 2019

O20	Understanding a Hydroformylation Catalyst the Produces Branched Aldehydes from Alkyl Alkenes	Paul Dingwall, Michael Buehl and Matt Clarke
O21	On the development of kinetic models for gold catalyzed HMF oxidation in basic medium	Arun Pankajakshan, Rebecca Engel, Sankar Meenakshisundaram, Donald Bethell, Graham Hutchings, Asterios Gavriilidis and Federico Galvanin
O22	CO2 hydrogenation to CH3OH over PdZn catalysts	Jonathan Esquius, Robert Armstrong, Hasliza Bahruji and Graham Hutchings
O23	Ni stabilised in La2Zr2O7: a robust catalyst for CO2 recycling	Estelle le Sache, Laura Pastor-Pérez, David Watson, Antonio Sepúlveda-Escribano and Tomas Ramirez-Reina
O24	Sustainable CO2 conversion over visible-light-responsive perovskites via artificial photosynthesis	Eduardo Morais, Kristy Stanley, Ravindranathan Thampi and James Sullivan
O25	Nanocatalysts from Ionic Liquid Precursors for the Direct Conversion of CO2 to Hydrocarbons	Nancy Artioli, Peter Nockemann and Callum Jeffrey
O26	Non-thermal plasma enabled CO2 methanation over zeolite supported Ni catalysts employing La as promoter: probing the reaction mechanisms using in-situ DRIFTS	Huanhao Chen, Yibing Mu, Xiaolei Fan and Christopher Hardacre
O27	Selective hydrogenation of sorbic acid over Pd and Pd-Re catalysts	Xiaohan Chen, Helen Daly, Haresh Manyar and Chris Hardacre
O28	Hydrogenation and low temperature hydrodeoxygenation of oxygen-substituted aromatics	Kathleen Kirkwood and David Jackson
O29	Preparation, Characterisation, and Testing of Supported Nickel Catalysts for Tetralin Hydrogenation	Ahmed Alasseel and David Jackson
O30	Hydrodeoxygenation of guaiacol over Pt/NC catalysts by in-situ generated hydrogen from water splitting	Wei Jin, Laura Pastor-Pére, Tomas Ramirez Rein and Sai Gu
O31	Inductive Heating Assisted Catalytic Hydrogenation of Naphthalene as a Model Compound of Poly-aromatics in Heavy Oil	Abarasi Hart, Mohamed Adam, John Robinson, Sean Rigby and Joseph Wood
O32	Bulk and surface properties of metal carbides: implications for catalysis	Matthew Quesne, Alberto Roldan, Nora de Leeuw and Richard Catlow

O33	Towards the Computational Rational Design of High-Performance Water Oxidation Electrocatalysts	Max García-Melchor, Michal Bajdich and Aleksandra Vojvodic
O34	Hydrogen adsorption on Transition Metal Carbides: A DFT study	Fabrizio Silveri, Matthew G. Quesne, Alberto Roldan, Nora H. De Leeuw and C. Richard A. Catlow
O35	Mesoporous titania thin films for photocatalysis	Genevieve Ososki and Philip Davies
O36	Dye sensitization of semiconducting Sn3S7(trenH)2 by ion exchange for photocatalysis	Mathias Hvid, Henrik Jeppesen and Nina Lock
O37	Nanoscale 3D elemental imaging and quantification to improve synthesis of Au@HgCdTe nanorods	Yi-Chi Wang, Thomas J.A. Slater, Xinyuan Li, Jiatao Zhang and Sarah J. Haigh
O38	Reduction of Methyl Orange in Presence of Silver-Pol(N-isopropylacrylamide-2-hydroxyethylmethacrylate-acrylic acid) Hybrid microgels Catalyst	Zahoor Farooqi, Robina Begum, Shumaila Batool and Khalida Naseem
O39	Enhanced Feedstock Recycling of Plastic Waste	Arthur Garforth, A Akah, A D Martin and J Hernandez-Martinez
O40	Influence of Anodic Potential Limit on the Electrocatalytic Performance of Size-Selected Platinum Clusters	Jo Humphrey, Patrick Harrison, Quanmin Guo, Richard Palmer and Andy Wain
O41	UiO-66 supported nickel catalysts for CO2 hydrogenation to methane assisted by non-thermal plasma	Yibing Mu, Huanhao Chen, Xiaolei Fan and Christophere Hardacre
O42	A newly-developed plug flow plasma DRIFTS cell for the in-situ investigation of plasma-assisted heterogeneously catalysed reaction	Cristina-Elena Stere, Sarayute Chansai, Rahman Gholami, Kanlayawat Wangkawong, Alex Goguet, Chris Hardacre and Burapat Inceesungvorn
O43	Sintering and Coking resistant Nickel/Zinc Oxide Yolk Shell Particles: Performance within the DRM reaction	Cameron Price, Laura Pastor-Perez, Tomas Reina and Jian Liu
O44	Efficient use of Rh via exsolution for application in automotive exhaust control	Chenyang Tang, Kelly Kousi, Dragos Neagu, Evangelos Papaioannou and Ian Metcalfe
O45	The Hydrothermal Growth of Metal Oxide Nanoparticles With Tailorable Morphololgies	Josh Davies, Philip Davies and M Sankar

O46	CO Binding and CO-induced Segregation of Highly Dilute Alloys: Investigating Nanoparticle Edges using Density Functional Theory	Konstantinos Papanikolaou, Matthew Darby and Michail Stamatakis
O47	Computational QM/MM and AIMD studies of the Methanol to Hydrocarbons process on zeolites H-Y and H-ZSM-5	Stefan Nastase, Alexander O'Malley, Andrew Logsdail and Richard Catlow
O48	Structural Geometry of Small α-NiMoO4 Nanoclusters Adsorbed on Al-PILC: a Combined EXAFS and DFT Studies	Ferensa Oemry, Anna Kroner, Indri Badria Adilina, Nino Rinaldi and Elizabeth Shotton
O49	Operando Kerr-Gated Raman Investigation of Methanol Conversion on Zeolites	Ines Lezcano-Gonzalez, Emma Campbell, Miren Agote-Aran, Emma Gibson, Alex Greenaway, Igor Sazanovich, Mike Towrie and Andrew Beale
O50	Experiment and simulation reveal how mutations in functional plasticity regions guide plant monoterpene synthase product outcome	Kara Ranaghan
O51	Hydrodeoxygenation of guaiacol as a lignin model compound over pillared clay supported NiMo catalyst	Indri Adilina, Nino Rinaldi, Sabar Simanungkalit, Fauzan Aulia, Ferensa Oemry, Ian Silverwood and Stewart Parker
O52	Active Site Hydration Governs the Stability of Sn-Beta during Continuous Glucose Conversion	Luca Botti, Daniele Padovan and Ceri Hammond
O53	Nitrogen Based Acidic Ionic Liquids for the Esterification of Glycerol with Acetic Acid	John Keogh, Manish Tiwari and Haresh Manyar
O54	Industrial Fertiliser Production and Performance	Daniel Holland
O55	Growth of carbon nanotubes with enriched chiral angles	Santiago Esconjauregui, Lorenzo D'Arsie, Hisashi Sugime, John Robertson
O56	FAU Y zeolites with superior mesoporosity for fluid catalytic cracking (FCC)	Xiaolei Fan
O57	Decomposition of hydrogen iodide over NiO/ZrO2 xerogel catalyst in sulfur-iodine cycle for the production of hydrogen	Ashok Bhaskarwar, Sony Chaddha, Divya Jyoti, Damaraju Parvatalu and Bharat Bhargav
O58	Chemical Equilibrium Analysis of Glycerol Steam Reforming to Hydrogen at Low Pressure	Ammaru Ismaila and Xiaolei Fan

UKCC 2019

O59	Phosgene Synthesis over an Activated Carbon Catalyst	Alastair Boyd, David Lennon and Don Jones
O60	Tin exchanged Tungstophosphoric acid supported on K-10 as catalyst for synthesis of n-Butyl levulinate from Furfuryl alcohol	Jennifer Dicks, Manish Tiwari, Vivek Ranade and Haresh Manyar
O61	Gas Phase Hydrogenation of Furaldehydes via Coupling with Alcohol Dehydrogenation over CeO2 supported Au-Cu	Fernando Cárdenas-Lizana, Chiara Pischetola, Laura Collado and Mark A. Keane